Sound level distribution and scatter in proportionate spaces[a)]

Stephen Chiles and Mike Barron[b)]
Department of Architecture & Civil Engineering, University of Bath, Bath, BA2 7AY, England

(Received 13 February 2004; revised 1 June 2004; accepted 1 June 2004)

Measurements have been conducted in two scale models of proportionate spaces each containing measures to promote a diffuse sound field. Contrary to classical statistical theory, it was found that reflected sound levels decrease with the distance from the source. Measured levels follow behavior predicted by a revised theory previously proposed for concert halls. The scatter of the measured reflected sound levels is shown consistently to exceed values predicted by Lubman/Schroeder's theory. However, it is demonstrated that this theory does accurately predict scatter of late sound levels when the early reflections are omitted. Investigation into the scatter of reverberation times shows that it is generally well predicted by Davy's theory. © *2004 Acoustical Society of America.*
[DOI: 10.1121/1.1775279]

PACS numbers: 43.55.Br, 43.55.Cs, 43.55.Mc, 43.55.Ka [NX] Pages: 1585–1595

I. INTRODUCTION

Practitioners regularly use classical statistical theory that predicts the same reflected sound level at all points in a room. For concert halls, measurement data[1,2] show this to be an oversimplification as the reflected levels significantly decrease with increasing distance from the source. From simple reasoning that the onset of reflected sound cannot occur prior to the arrival of the direct sound, Barron and Lee[2] developed a revised theory that predicts the average behavior of sound levels in concert halls more accurately. So far this revised theory has only been applied to auditoria, where there is a particular acoustic environment with virtually all the acoustic absorption (the audience) on one surface. Variations of revised theory have been proposed for application in reverberation rooms[3] and specific types of churches.[4,5]

A diffuse sound field is taken as the reference condition for room acoustics and a model investigation is reported here that tests whether this revised theory is applicable to proportionate spaces designed to have diffuse sound fields. Two commonly accepted ways to promote a diffuse sound field are nonparallel geometry and scattering surfaces. The results given below are for measurements in two physical acoustic scale models: one with nonparallel geometry and the other with scattering surfaces.

II. SOUND LEVEL IN ROOMS

A. Classical theory

Sound received in a space from a single source can be split into a direct and reflected component. The prediction of the direct component is common in all approaches and accepted as giving an accurate result. The following discussion considers only the reflected component, for which the various prediction methods give significantly different results. To obtain the total sound level by any of these methods would require the addition of the direct component to the expressions given below for the reflected component.

Equation (1) is the classical statistical expression for reflected sound energy,

$$\frac{\overline{p^2}}{\rho c} = \frac{4W}{A}, \tag{1}$$

where p is the sound pressure, ρ is the density of air, c is the speed of sound in air, W is the sound power of the source and A is the total acoustic absorption in metric Sabines. This equation does not account for receiver (or source) locations and it therefore predicts the same reflected sound level throughout a space. Equation (1) is usually derived through consideration of the balance of acoustic energy introduced into and absorbed in a room. An alternative derivation of reflected sound energy can be based on an image model, which predicts exponentially decaying sound in a space.[6] In this model, the reflected level in Eq. (1) is obtained by summing the energy arriving at a point, from the moment of direct sound leaving the source to infinite time. Implicit in this alternative derivation is that the onset of the reflected sound occurs simultaneously at all points throughout the space at the moment the direct sound is emitted.

B. Revised theory

Revised theory[2] can be derived by reasoning that, as reflected sound cannot arrive earlier than direct sound, the arrival time of the direct sound can also be taken as the onset time of the reflected sound at that location. During a sound decay the instantaneous sound level at any moment is still taken to be the same throughout the space and the sound is still taken to decay exponentially. Therefore, the later the delayed onset the lower the reflected sound level will be at a given point. This is illustrated in Fig. 1, which shows three idealized decay curves for receiver positions (A, B, and C) located progressively farther away from the source. The direct sound is emitted from the source at time $t=0$ and reaches each of the receivers at times t_A, t_B, and t_C, respec-

[a)]Portions of this work were presented in "Distribution of reflected levels in rooms with diffuse sound fields," Proceedings of the 18th International Congress on Acoustics, Kyoto, April 2004, and "Sound level distribution in rooms: is it really the same everywhere ?," Proceedings of the Institute of Acoustics, Oxford, November 2003.

[b)]Electronic mail: M.Barron@bath.ac.uk

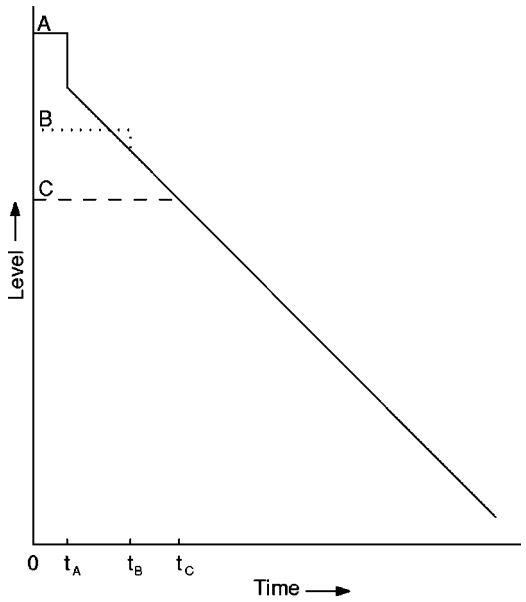

FIG. 1. Decay curves at three source–receiver distances according to revised theory. Here, $t=0$ is the time when the sound is emitted from the source and times t_A, t_B, and t_C are when the direct sound reaches receivers A, B, and C, respectively.

tively. At times later than the direct sound arrival at the farthest position, the decay curves all coincide as the instantaneous level is the same throughout the space. Moving away from the source, the direct sound becomes less prominent until at receiver C it is not visible in the decay trace. The image model using these revised integration times gives a revised value for reflected energy:

$$\frac{\overline{p^2}}{\rho c}=\left(\frac{4W}{A}\right)e^{-0.04r/T}, \tag{2}$$

where r is the source–receiver distance in meters and T is the reverberation time in seconds. Barron and Lee[2] examined the regression of measured sound levels against the source–receiver distance for 17 concert halls. From this measurement data it was apparent that in concert halls there is generally a linear correlation with distance and, extrapolating from the regression lines, Eq. (1) correctly predicts the reflected sound level close to the source. An analysis showed that the average behavior in concert halls was well described by Eq. (2).

For practical application, revised theory, Eq. (2), can be rewritten in terms of the reflected sound pressure level, L_{p_r}, and sound power level, L_W:

$$L_{p_r}=L_W+10\log(A)+6-0.174(r/T), \tag{3a}$$

or, using the Sabine equation,

$$L_{p_r}=L_W+10\log(T)-10\log(V)+14-0.174(r/T), \tag{3b}$$

where V is the room volume in m^3.

It can be seen that Eq. (2) differs from Eq. (1) by the factor $e^{-0.04r/T}$, which when expressed in decibels gives a decrease in the reflected sound level at a rate of 0.174/T dB/m as one moves away from the source. The maximum effect due to revised theory is thus a function of $r_{\max}/T$. If we take a cube of side z, the length of the diagonal is $\sqrt{3}z$, and $r_{\max}$ will be roughly 75% of this, namely $0.75\sqrt{3}z$. According to the Sabine equation $T=0.16V/S\overline{\alpha}=0.16z^3/6z^2\overline{\alpha}$, giving $0.174r_{\max}/T=\text{const.}\overline{\alpha}$, where S is the total area of the room surfaces in m^2 and $\overline{\alpha}$ is their average absorption coefficient. For spaces with the same proportion, the maximum revised theory effect is thus a function of $\overline{\alpha}$ alone, not size, for instance. It can be seen above that the value of the constant depends on the proportions of the space; for a cube it is 8.5, for a double cube 10.0, and for the models in this investigation it is approximately 9. This means that the maximum revised theory effect, $\Delta G_{r,\max}$, for these models is

$$\Delta G_{r,\max}\approx 9\overline{\alpha}\ \text{dB}. \tag{4}$$

For a maximum revised theory effect of, say, 3 dB, an average absorption coefficient of around 0.33 is required. With a small average absorption coefficient Eq. (2) gives very similar results to Eq. (1). For spaces such as reverberation chambers (typically $\overline{\alpha}=0.03$) there is little benefit in using Eq. (2) rather than Eq. (1), whereas for concert halls, which have a higher average absorption coefficient, there is a significant difference between the two results, by up to 3 dB at remote seats.

C. Alternative theories

Vorländer[3] proposed that, rather than starting the onset of reflected sound at the arrival of the direct sound, it should be started at the arrival of the first reflection. It can be shown that the average arrival time of the first reflection is the time for sound to travel the mean free path, 4 V/S. If this is substituted for r in Eq. (2) and the reverberation time, T, is expressed as 0.16 V/A, then the constants and the volume cancel out to leave

$$\frac{\overline{p^2}}{\rho c}=\left(\frac{4W}{A}\right)e^{-A/S}. \tag{5}$$

Vorländer went on to show that if the Eyring absorption exponent is used, ignoring air absorption so that $A=S\ln(1-\overline{\alpha})$, then Eq. (4) can be written as

$$\frac{\overline{p^2}}{\rho c}=\left(\frac{4W}{A}\right)(1-\overline{\alpha}). \tag{6}$$

This was proposed primarily for reverberation chambers where the measurement results are spatially averaged. Equation (6) is a well-established and commonly used modification of Eq. (1), notionally to account for a decrease in the reflected level due to sound absorbed at the first reflection, but there has been no robust derivation of this prior to Vorländer's work.

Several recent measurement exercises in religious buildings[4,5,7,8] also show reflected sound levels to generally decrease with an increasing source–receiver distance, contrary to classical theory, Eq. (1). However, the reflected levels in these religious buildings generally fall below those predicted by revised theory. In their study of Gothic-Mudejar churches Sendra *et al.*[4] introduce an adjustment parameter, ß, to Eq. (2), giving

$$\frac{\overline{p^2}}{\rho c} = \left(\frac{4W}{A}\right) e^{-\beta r/T}. \quad (7)$$

For each octave band, average values of ß are empirically derived from measurement data and Eq. (7) is proposed for general use in this specific type of church. During a study of Apulian Romanesque churches, Cirillo and Martellotta[5] theoretically derive an alternative adjustment to Eq. (2). Like Vorländer, they identify that the onset of reflected sound does not in reality start at the arrival time of the direct sound. Their solution is to assume that the delay is proportional to the source–receiver distance and derive a correction on this basis. They also derive a correction to account for the specific early reflection pattern. While these corrections do not rely on empirical data, their formulation makes many approximations and results in a complex set of expressions only tested for these Apulian Romanesque churches.

D. The present study

Revised theory, Eq. (2), does not account for the distribution of absorption or room geometry and defines receiver positions solely in terms of their distance from the source. These assumptions allow revised theory to retain most of the simplicity of the classical statistical formula, with no new parameters required (source–receiver distance is already needed for calculation of the direct sound level). As previously mentioned, it has been shown to be significantly more accurate than classical theory for concert halls. The question behind this investigation is whether revised theory can also give sufficiently robust predictions for other spaces and specifically in the reference condition of a proportionate space with a diffuse field. Alternative theories, illustrated by those presented above, tend to have a limited application and introduce such complexities that they represent a more detailed level of analysis that would perhaps be better handled by standard computer modeling packages.

III. MODELING

A. Measurement system

The use of physical scale modeling is an established technique in room acoustics.[9] For this investigation, key characteristics of the University of Bath's modeling system were reviewed: verification measurements were made of transducer directivity, spark source linearity, and air absorption corrections. In this investigation a greater accuracy is desired than is needed for say auditorium modeling. The microphone directivity and air absorption are discussed below. Measurements of the spark source showed it to have nonlinear propagation to a distance of approximately 100 mm. To ensure that measurements are only in the region of linear propagation, a minimum source–receiver distance of 200 mm (5 m full-size at a scale of 1:25) is used in this investigation. As shown previously by Barron,[10] the energy of the spark source over the frequency range used in this investigation increases at approximately $+9$ dB/octave. A first-order low pass filter (-6 dB/octave roll-off) is included in the analysis system to attenuate the high frequencies and effectively reduce the slope of the spark spectrum to approximately $+3$ dB/octave.

The modeling system uses two 1/8-in. microphones. To account for slight variations in the spark source level, the energy of the direct sound is measured with the second reference microphone. This also allows for situations where the direct sound is obscured to the first microphone. To reduce the effect of any variation in the spark source directivity, all results presented are average values from the individual analysis of three separate sparks. Variations of the spark source level/directivity are not significant in the results presented below. For both models, the spark source and two microphones are located at the bottom of adjustable height tubes held in randomly distributed sockets on the models' top surfaces. Spark discharges are directly recorded to obtain impulse responses, which are then stored and sequentially filtered in third-octave/octave bands. All normal room acoustics parameters are obtained using standard reverse integration, with a noise and tail correction to extend the dynamic range available. An iterative method[11] is used to determine the decay/noise cross-point and the decay is truncated at 5 dB above this point. The energy that would exist from a linear decay after this truncation point is added to the total energy of the truncated decay when calculating the reverse integrated response. The average noise energy is determined from the end section of the measurement and is subtracted from the pressure squared impulse response. Reverberation time T_{20} is obtained from the slope of the reverse integrated decay curve's regression line from 5 dB to 25 dB below the initial level.

The upper frequency used in the models is determined by the directivity of 1/8-in. microphones which, the manufacturer's data shows and the verification measurements confirmed, are omnidirectional to within ± 1 dB up to the 16 kHz third-octave band. The spark source was designed to have maximum energy at a frequency slightly above 16 kHz, so that its spectrum changes at a constant rate ($+9$ dB/octave) over the measurement range. The lower frequency limit (5 kHz third-octave band) is determined by the energy from a single spark that still maintains a signal-to-noise ratio of at least 25 dB. In the context of this investigation the absolute full-size equivalent frequencies are not critical. For convenience, a scale factor of 1:25 was chosen, since the models then represent realistic spaces and it gives results in a familiar frequency range: 250 Hz and 500 Hz octave bands. To avoid confusion, the later results and discussion are always for the full-size equivalent frequencies and distances.

To reduce air absorption at high frequencies, previous modeling at the University of Bath has been conducted in dry air or nitrogen. However for this investigation, the relatively large models make these options less practical. The measurements presented here were made in air with numerical corrections for absorption according to ISO 9613-1.[12] The validity of the correction procedure used is demonstrated in Fig. 2, which shows sample decays from measurements that were conducted in air and then repeated in nitrogen. The graph shows the same measured decay in air with

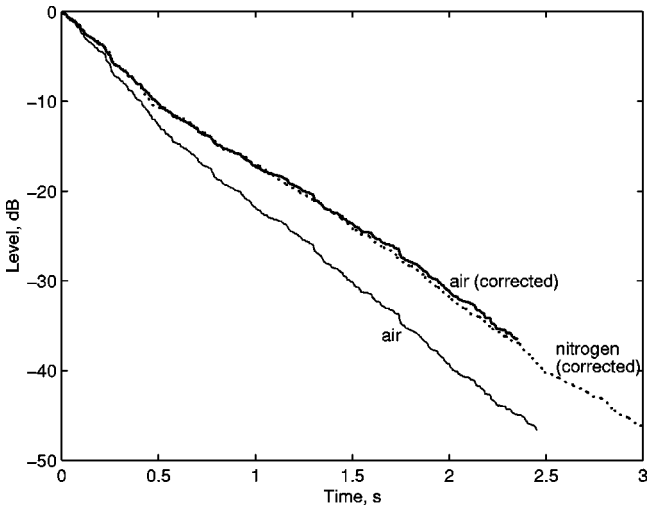

FIG. 2. Reverse integrated sound level decay curves for the same source–receiver combination when the model is filled with air (solid lines) and filled with nitrogen (dotted line). The decay in air is shown uncorrected for air absorption and corrected using the equations from ISO 9613-1 to standard atmospheric conditions: 20 °C, 50% R.H., 1013.25 mb. The decay in nitrogen has been corrected for air absorption but the magnitude of the correction is minimal.

and without correction for air absorption. When the correction has been applied the decay in air can be seen to be close to the decay measured in nitrogen. The decay in nitrogen has also been corrected for air absorption but the adjustment is very minor. These graphs illustrate that a penalty of measuring in air rather than nitrogen (or dry air) is that there is a significant loss of dynamic range in the corrected decay.

B. Model constructions

Figures 3 and 4 show the two models used in this investigation, which are both of similar size with the longest dimension just over 1 m actual size. Model 1 has flat surfaces and three of the walls are angled by 5° (one from each pair of opposite walls). Model 2 is rectangular and has highly irregular surfaces comprising scattering hemicylinders and deep absorptive devices. Certain ratios of dimensions for rectangular spaces encourage a good distribution of modes and hence promote a diffuse sound field.[13] Two of these ratios are the basis for the two models: 1/0.7/0.59 (Model 1), 1/0.83/0.65 (Model 2). In Model 1, the ratio is only used to obtain a reasonable starting point as the walls are angled to promote the uniform distribution of modes. In Model 2 there are not simple internal dimensions, due to the depth of the irregular surfaces, and there is some deviation from the chosen ratio. Model 1 is constructed from 9 mm thick, melamine faced, medium density fiberboard. The melamine facing gives a smooth, acoustically reflective finish. Model 2 is constructed from 12 mm thick plywood but the internal surfaces are completely covered with the absorbing and scattering finishes described below.

FIG. 3. Photograph of Model 1. The rear, left, and bottom surfaces are angled at 5° from parallel with their opposites. The surfaces are acoustically reflective other than the squares seen in the photograph, which are a velvet material providing acoustic absorption. The front surface is transparent acrylic. Transducers are suspended from the top surface.

FIG. 4. Photograph of Model 2 during construction. The black hemicylinders are 75 mm diameter rainwater guttering used to provide a scattering surface. In the completed model the wells between the guttering are covered with a velvet material.

From Eq. (4) it can be seen that revised theory only predicts a significant difference (>1 dB) from classical theory, at the maximum source–receiver distance, when the average absorption coefficient, $\overline{\alpha}$, in a proportionate space is greater than about 0.1 ($\overline{\alpha}$ is typically 0.3 in concert halls). For the purposes of testing revised theory a reasonable amount of absorption is therefore included in both models. This absorption is evenly distributed on all surfaces to further promote a diffuse sound field. Figure 3 shows Model 1

TABLE I. Dimensions and average measured reverberation times of Models 1 and 2. The dimensions are given as the full-size equivalent values for the scale of 1:25. Neither of the models are simple cuboids and the linear dimensions given are the maximum values in the case of Model 1 and the values inside the scattering/absorbing surfaces in Model 2. The volume for Model 1 is that calculated by the acoustic computer model and for Model 2 it is the volume inside the scattering/absorbing surfaces.

	Full-size equivalent dimensions				Rev. Time	
	Volume	Length	Width	Height	250 Hz	500 Hz
Model 1	9798 m^3	30.0 m	17.7 m	21.0 m	3.39 s	1.88 s
Model 2	9453 m^3	26.2 m	16.7 m	21.7 m	1.24 s	1.32 s

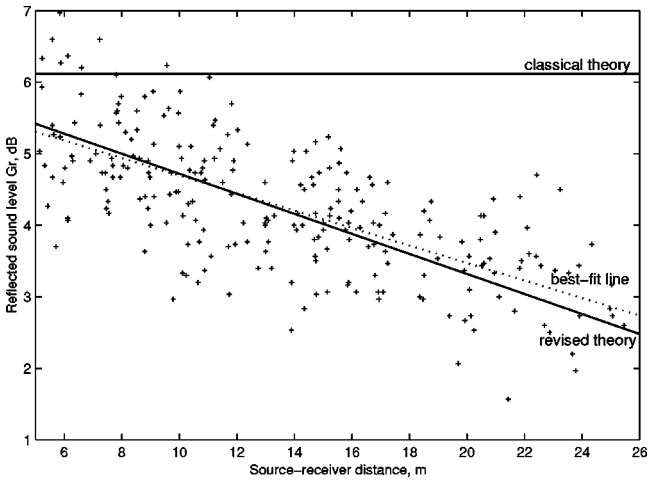

FIG. 5. Reflected sound level measurements plotted against the source–receiver distance for the 500 Hz octave band in Model 2. Lines are shown for the theoretical values of G_r according to classical and revised theories and also the best-fit line through the measurement data.

with 200 mm square patches of absorbing velvet material. The average absorption coefficient in Model 1 is 0.16 to 0.29 at the measurement frequencies. Figure 4 shows Model 2 during construction; when completed, the 40 mm deep wells, between the black hemicylinders, are covered by strips of velvet material as porous absorbers. The average absorption coefficient in Model 2 is 0.42 to 0.45. Previous measurements of hemicylinders[14] show the scattering coefficient, plotted against frequency, to have a small value at low frequencies and then rise steeply to a fluctuating plateau. The frequency at which the steep rise in scattering coefficient occurs is inversely proportional to the radius of the hemicylinders. For Model 2, the hemicylinders were selected on the basis of a practical material (rainwater guttering) with a radius large enough that the steep rise in scattering coefficients occurs below the measurement frequencies. Full-size equivalent dimensions of the models and the average measured reverberation times are given in Table I.

IV. SOUND LEVEL DISTRIBUTION

A large number of measurements were made in both models. In room acoustics the parameter G is defined as the total sound level relative to the direct sound at 10 m from the source.[15] This investigation is concerned only with reflected sound and not the total sound which includes direct sound. The parameter G is modified here by excluding the first 5 ms, which contains the direct sound, resulting in just the reflected sound level, denoted G_r,

$$G_r = 10 \log_{10} \frac{\int_5^\infty p^2(t)dt}{\int_0^5 p_{10}^2(t)dt}, \tag{8}$$

where p is the pressure at the receiver position and p_{10} is the pressure that would occur at a position 10 m from the source. Measurements were taken at 156 source–receiver pairs in Model 1 and 240 source–receiver pairs in Model 2. Figure 5 shows the measured G_r values plotted against distance for the 500 Hz octave band in Model 2. There are no measurements closer than 5 m to the spark source to avoid nonlinear propagation. Results in Model 1 and at 250 Hz in Model 2 have the same overall trends seen in Fig. 5. For both models and octave band frequencies, statistics of the regression lines compared to the revised theory predictions are given in Table II.

From these results it appears that revised theory is substantially more accurate than classical theory for predicting sound levels in proportionate spaces with diffuse sound fields. The scatter of sound levels about the revised theory prediction line, seen in Fig. 5, is discussed in Sec. VI. For each model and each frequency band there is clear evidence that the reflected sound level decreases with the distance from the source. Although the best-fit lines through the data often vary slightly from revised theory, no systematic difference was identified and the mean differences are small. Within 95% confidence limits, the differences between the slopes and intercepts of the best-fit lines and the revised theory predictions are not statistically significant except in the case of the slopes of the lines in Model 2. These slopes fall outside the 95% confidence limits but the difference is not of practical significance and would not be of statistical significance were it not for the large number of data points (240). The close agreement between measured levels and revised theory is an important result with major implications. For many practical spaces, where acousticians are currently using classical theory to predict sound levels, there is now a firm basis for the adoption of revised theory.

V. SOUND LEVEL DECAY CURVES

A further test of revised theory can be made by examining superimposed decay curves measured in the models. According to revised theory, the instantaneous level in a space

TABLE II. Statistics for sound level measurements and predictions in Models 1 and 2. For measurements, the statistics are taken from the linear regression line of reflected sound levels against the source–receiver distance and for predictions the mean level and slope are taken from the revised theory line against the source–receiver distance. The mean levels are the reflected sound level at the mean measurement distance, which happens to be the same in both models, 13.4 m.

		Mean level (dB)			Slope (dB/m)		
		Measured	Predicted	Difference	Measured	Predicted	Difference
Model 1	250 Hz	9.7	9.7	0.0	−0.05	−0.05	0.00
	500 Hz	6.9	6.6	−0.3	−0.08	−0.09	0.01
Model 2	250 Hz	4.2	4.6	0.4	−0.17	−0.13	−0.04
	500 Hz	4.3	4.2	0.0	−0.12	−0.14	0.02

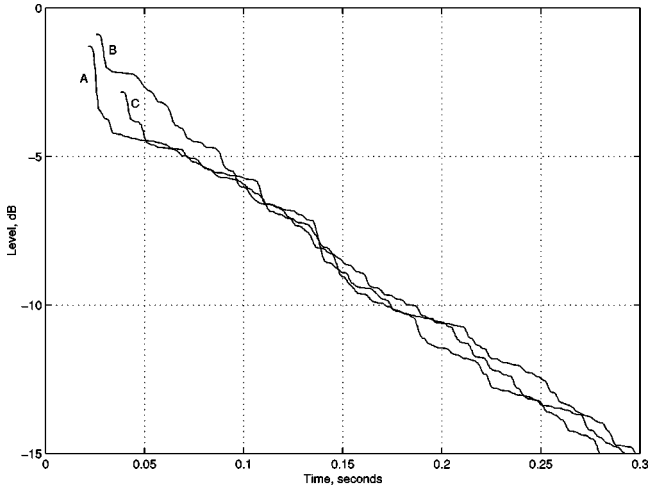

FIG. 6. Initial part of the reverse integrated (Schroeder) decays for three receiver positions. The moment when sound was emitted from the source is $t=0$ on the time axis.

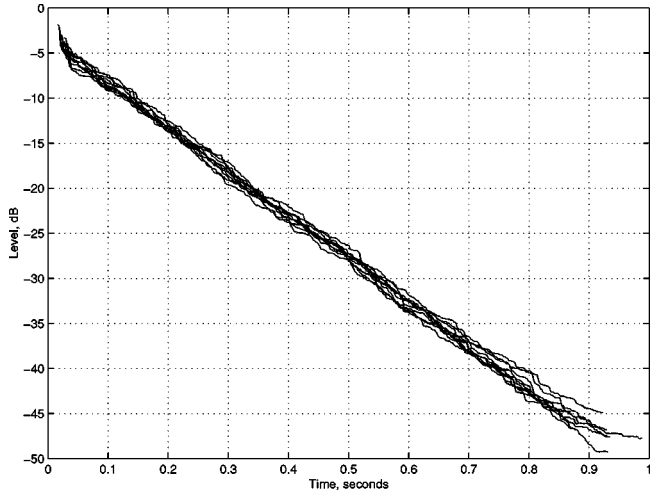

FIG. 7. Reverse integrated decays for ten receiver positions with the same source position in Model 2 at the 500 Hz octave band. The moment when sound was emitted from the source is $t=0$ on the time axis.

is the same at all positions during a sound decay. Therefore, as shown in Fig. 1, the measured sound level decay curves should coincide if they are each plotted with $t=0$ set as the time the source pulse is emitted. Normally individual decay curves are displayed starting at 0 dB. However, to compare different curves here, the magnitude of the start points are determined from the total measured sound level, G, at each position.

Figure 6 shows the initial part of three sound decay curves for the 500 Hz octave band in Model 2 at three receiver locations and the same source position. The three curves start at different times according to their source–receiver distances (7.5 m, 8.8 m and 13.0 m) and different levels in proportion to the measured total sound levels. Curve B has several strong early reflections visible as steps in the decay curve from the start point up to around 100 ms. Curve A has fewer early reflections which leaves the initial step of the direct sound more prominent. Due to these differences in early reflections, curve B has a slightly higher total level than curve A despite being marginally farther away from the source. However, although curve B is above curve A up to around 100 ms, they then converge, showing the later reflected sound to be uniform throughout the space. Position C is at a greater distance from the source than A or B and, as predicted by revised theory, has a correspondingly lower total level, although it converges with the other curves after the early reflections. The fact that the three curves converge is further evidence in support of revised theory. The differences in total levels show that generally the total levels decrease with an increasing source–receiver distance (curve C is lower than curves A and B) but there are minor fluctuations within this pattern (curve B is slightly higher than curve A).

Figure 7 shows the full decay curves measured for ten receiver positions with the same source position. These curves have been time and level aligned as described above. For most of the decay, the curves are reasonably close although towards the end the curves diverge. Investigations have shown this divergence at the end to be caused primarily by inaccuracies inherent in noise/tail correction to extend the measurement dynamic range (without any noise/tail correction the divergence would be greater). In the region where the curves are reasonably closely aligned, there is still some variation seen in Fig. 7. This has been quantified by the standard deviation of the decay curves' instantaneous level at each time step, for each model, source position and frequency band. In all cases, the standard deviation of the curves is greater at the start of the decay, due to direct sound and early reflections illustrated in Fig. 6, and at the end of the decay, due to the noise/tail correction. In between these regions, the average standard deviation in Model 1 is 0.65 dB for the 250 Hz octave band and 0.59 dB at 500 Hz. The values in Model 2 are 0.74 dB (250 Hz) and 0.57 dB (500 Hz). For Model 2, these values are very close to the theoretical standard deviations of reflected sound levels discussed below in Sec. VI. For Model 1, the values are higher than the theoretical standard deviations by 0.15–0.19 dB, which may be due to an insufficiently diffuse sound field, as discussed in Sec. VIII.

VI. SOUND LEVEL SCATTER

For the measured data, despite the close agreement of the average behavior with revised theory, it can be seen in Fig. 5 that there is significant scatter of the results around the best-fit line. The same is true at both frequency bands in both models and is partly explained by the theoretical fluctuation of sound levels within a space. This was investigated many years ago by Lubman[16] and Schroeder,[17] who both arrived at expressions that led to the following approximate equation for the standard deviation of sound levels measured in a room:

$$s_{G_r} = \frac{4.34}{\sqrt{\left(1+\left(\frac{BT}{6.9}\right)\right)}}\,dB, \tag{9}$$

where B is the bandwidth and T is the reverberation time. The derivation for this theoretical standard deviation starts

TABLE III. The scatter of reflected sound levels, measured as the standard error taken from the linear regression of the measured levels against the source–receiver distance, and predicted as the standard deviation using Eq. (9).

		Measured Standard Error	Predicted Standard Dev.
Model 1	250 Hz	0.58 dB	0.46 dB
	500 Hz	0.63 dB	0.44 dB
Model 2	250 Hz	0.99 dB	0.74 dB
	500 Hz	0.70 dB	0.54 dB

with Eq. (1) and the assumption that there are only *random* variations in level with the receiver position. The magnitude of the random variations is obtained by considering the steady state frequency response for a room to be a complex Gaussian process and the magnitude squared of the frequency response to be exponentially distributed.[17] The theory was originally only considered in the context of reverberation rooms. In such spaces it has been shown in Sec. II that the low average absorption coefficient means that revised theory would predict a negligible level variation with the source–receiver distance (the same result as classical theory). However, in the current investigation the standard deviation would also include the intrinsic variation of sound levels with the source–receiver distance, which was not accounted for in the derivation of Eq. (9). An alternative measure of scatter adopted here is to use the standard error taken from the linear regression of the measured reflected sound levels against the source–receiver distance. The use of standard error in place of standard deviation does not have a theoretical derivation, but in the absence of an equation for sound level scatter that accounts for the sound level decrease with distance, Eq. (9) used in this way gives useful values for comparison.

The data in Table III show that the standard errors for all measurements are consistently higher than the theoretical standard deviations. To explore the validity of Eq. (9) further, it is necessary to use data with a wider range of the two variables: reverberation time and bandwidth. This data was available from measurements made during the preparation of Model 1. The absorbing patches were originally added in three stages, with measurements made at each stage, giving results for a wide range of reverberation times. The last of these stages with 39 patches of absorption was the final condition for the main testing of Model 1. These impulse responses have been analyzed for the two octave bands at 250 Hz and 500 Hz and the six third-octave bands from 200 Hz to 630 Hz, giving a range of bandwidths. The standard errors for these measured sound levels are plotted in Fig. 8 against the predicted standard deviation. Figure 8 shows a general agreement between the measured standard error and predicted standard deviation, although it also highlights the consistent deviation at the two octave bands used in this study: the 250 Hz and 500 Hz octave bands (on the left of each set of points).

The theoretical model, Eq. (9), originated for reverberation rooms with low average absorption, whereas the spaces studied here have average absorption coefficients similar to

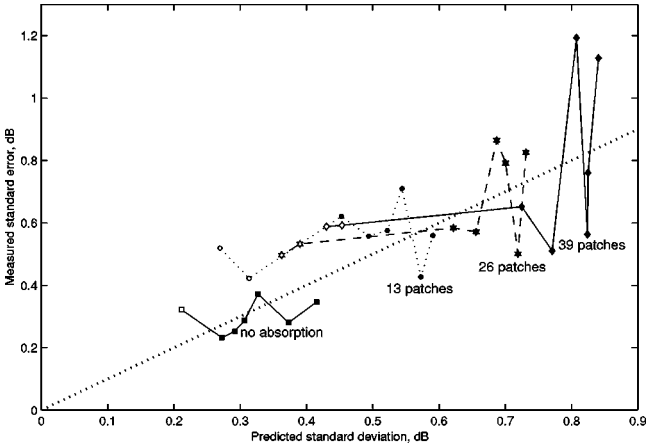

FIG. 8. Measured standard error plotted against the predicted standard deviation of reflected sound levels in Model 1 with four different amounts of absorption. In each set of data, the two left hand points with hollow symbols are for the 500 Hz and 250 Hz octave bands and the other six points to the right with solid symbols are for the third-octave bands from 630 Hz to 200 Hz. There is an exception for the set of data on the left, ''no absorption,'' where there is no 500 Hz octave band point. The straight dotted line is for equal predicted and measured values.

''real world'' rooms. However, even in a reverberation room, Lubman's measured standard deviations of sound level[18] consistently exceed the theoretical values by a similar percentage to that found in this investigation. The significant discrepancies found with standard deviations/standard errors of measured steady-state reflected sound levels indicate that the theory does not provide a reliable method for predicting this quantity. However, there is good agreement with average standard deviations of instantaneous late sound levels, presented above in Sec. V for Model 2.

The measured values for the late sound in Sec. V were obtained by calculating the average standard deviation of instantaneous sound levels for all receiver positions at each time step in the middle portion of the decays. As expected, very similar values are obtained in Model 2 by calculating the standard error against the source–receiver distance for the total late sound levels after 200 ms from the arrival of the direct sound. All these values are given in Table IV and show good agreement between the two different forms of analysis used and the theoretical predictions. For both analysis techniques, the choice of time window over which the statistics were obtained was determined experimentally. It can be seen in Fig. 6 that three of the decay curves converge after approximately 100 ms and it was found through an examination of statistics for 240 curves that they had all converged

TABLE IV. The scatter of late sound levels in Model 2. The theoretical standard deviation is from Eq. (9). The measured decays have been analyzed taking the average standard deviation, SD, of instantaneous sound levels during the middle portion of the decay and the standard error, SE, for correlation of the total late sound after 200 ms against the source–receiver distance.

	250 Hz	500 Hz
Theoretical Standard Deviation	0.74 dB	0.54 dB
Average SD of instantaneous levels	0.74 dB	0.57 dB
SE of late sound levels after 200 ms	0.79 dB	0.54 dB

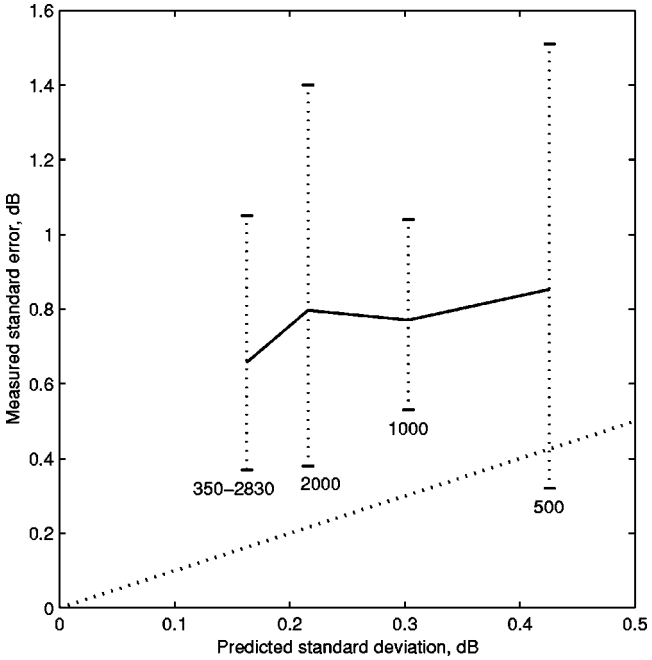

FIG. 9. Average measured standard error plotted against the predicted standard deviation of reflected sound levels in 16 concert halls. Error bars show the maximum and minimum values. The three right hand points are the average standard errors in the 2 kHz, 1 kHz, and 500 Hz octave bands and the left-hand point is the standard error for the average of these three bands. For simplicity, the reverberation time for the theoretical values at these three frequency bands has been taken as 2 seconds for all the halls. The straight dotted line is for equal predicted and measured values.

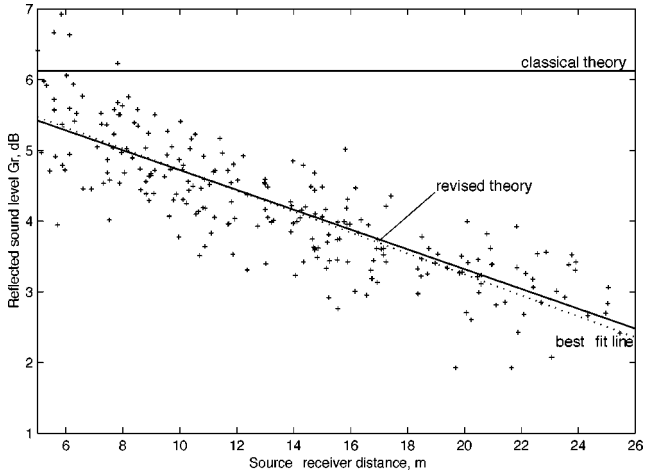

FIG. 10. Reflected sound level according to computer prediction plotted against the source–receiver distance for the 500 Hz octave band in Model 2. Lines are shown for the theoretical values of G_r according to classical and revised theories and also the best-fit line through the measurement data. The computer predictions in this graph are for the same scenario as Fig. 5 for the scale model measurements.

by around 200 ms for the 250 Hz octave band and 150 ms for the 500 Hz octave band. The statistics are not unduly sensitive to slight variations in these timings and, for the 500 Hz octave band, the standard error of the total late level after 150 ms is only 0.01 dB different from the value given for 200 ms. At the other end of the time windows, the average standard deviation of instantaneous levels did not include values after the decay curves started to diverge but the total late levels include the entire decays after 200 ms. This does not however, significantly affect the results as the end of the decays contribute little to the total late levels.

The good agreement between measurements and predictions seen in Table IV indicates that Eq. (9) does accurately predict the scatter of sound levels in the decaying sound field. It can be seen from examination of the decay curves that, on average, they do coincide for reflected sound, although there is always some variation of the instantaneous levels. It has been found that the magnitude of this variation is consistent over the length of the decays, apart from the initial section, which is controlled by the early reflections (divergence at the end of the curves is attributed to measurement/analysis issues and not the physical decays). This investigation has shown that the theory presented, Eq. (9), does accurately predict the variations during the main part of the decay but does not account for the variation of early energy. The total reflected sound level in most spaces is highly dependent on early reflections, thus making the theory limited in potential applications.

For reference, Fig. 9 shows the mean and range of standard errors of reflected sound levels measured at audience positions in 16 concert halls for the 500 Hz, 1000 Hz, and 2000 Hz octave bands. The left-hand bar in Fig. 9 is the standard error of the reflected sound levels averaged over these three octave-bands (350–2830 Hz). Concert halls, having a very uneven distribution of absorption (concentrated on the floor) and complicated geometries, could be expected to have a less uniform sound field than Models 1 and 2, and this is borne out by the high standard errors seen in Fig. 9 relative to predictions according to Eq. (9).

VII. COMPUTER MODELING

In parallel with the scale modeling, the two model spaces have been analyzed in a computer simulation (CATT-Acoustic). The simulation results for the 500 Hz octave band in Model 2 are shown in Fig. 10, which is equivalent to Fig. 5 for the scale model. For the predictions presented in Fig. 10 a scattering coefficient of 0.5 was used for all surfaces in the computer model. However, as the absorption in the model is evenly distributed the scattering coefficient has negligible effect on the results.

The overall trend of decreasing sound levels with increasing source–receiver distance in Fig. 10 is very similar to that seen in Fig. 5, although the slope of the decrease is higher for the computer simulation. Table V lists the scatter of sound levels measured in the scale model and predicted by the computer simulation for Model 1. It can be seen that there is significantly less scatter of reflected sound levels in

TABLE V. Scatter of reflected sound levels in Model 1 for 52 receiver positions and a single source position.

	250 Hz	500 Hz
Theoretical Standard Deviation	0.46 dB	0.44 dB
Standard Errors:		
Scale model measurements	0.56 dB	0.56 dB
Computer model predictions	0.19 dB	0.46 dB
Computer model with phase	0.71 dB	0.70 dB

TABLE VI. Relative standard deviations of reverberation times (T_{20}) measured in the two models and predicted using Eq. (10).

		Measured	Predicted
Model 1	250 Hz	6.4%	3.7%
	500 Hz	5.3%	3.5%
Model 2	250 Hz	5.7%	6.0%
	500 Hz	3.8%	4.3%

the computer simulation than for the scale model measurements, with a standard error even lower than the theoretical standard deviation at 250 Hz. The reason for the lesser scatter was assumed to be due to the exclusion of phase in the computer modeling. To test this hypothesis, data for one source position and 52 receivers in Model 1 were reanalyzed using the output from an auralization module, which includes an approximation for phase information. To enable realistic auralization, this module uses a synthesized phase and maintains the correct reflection density throughout the decay. To compute in a reasonable time, late energy is not processed as discrete reflections and for this late energy the application of the synthesized phase is approximate.

Table V shows that when the phase approximation is included it does significantly increase the reflected sound level scatter and demonstrates that the original lower scatter is due to the omission of phase in the standard calculations. However, the scatter with the phase approximation is slightly higher than the measured scatter due to the technique used to process the late sound discussed above. An examination of the correlation between computer predictions and scale model measurements has shown that the inclusion of phase approximations in this computer model does not appear to improve the accuracy of the individual sound level prediction at a particular receiver. Also, as seen in Table V, the omission of phase is only significant at the lower frequency, whereas most users of routine computer models are primarily interested in results at the midfrequencies.

VIII. REVERBERATION TIME SCATTER

Initially it was suspected that a reason for the measured sound level scatter being higher than predicted could be due to the sound field being insufficiently diffuse. A possible measure of sound field diffusion is the scatter of the reverberation time, expressed as the relative standard deviation. Davy *et al.*[19,20] derived a theoretical value of this quantity, which for impulse response measurements of a 20 dB decay is

$$\frac{\sigma(T_{20})}{\overline{T_{20}}} = \frac{0.96}{\sqrt{BT}}. \tag{10}$$

In this equation, the bandwidth, B should be the statistical bandwidth rather than the nominal or effective bandwidth.[21] The filters used in this investigation are 5th order Butterworth and the statistical bandwidths for them are obtained by increasing the nominal bandwidths by 11%.[22]

Table VI shows the measured and predicted relative standard deviations of reverberation times for the two models. It can be seen that for Model 2 there is reasonable agreement between measurements and predictions, as has been found previously in reverberation rooms by Bartel and Magrab,[23] Flenner *et al.*,[24] and Warnock.[25] The slight overestimation by Eq. (10) has been previously reported by Davy.[21] However, for Model 1 the measured values are significantly larger than predictions. Table VII lists standard deviations for Model 1 as the absorptive finishes were progressively introduced. This shows that the relative standard deviation of reverberation times is following the behavior predicted by Eq. (10) in that it increases with decreasing reverberation time but the magnitude is consistently greater than predictions. It is thought that Model 1 has an insufficiently diffuse sound field with excessive spatial variations, which have resulted in the discrepancies between measurements and predictions. This is discussed further later.

TABLE VII. Relative standard deviations of reverberation times (T_{20}) measured in and predicted for Model 1 as absorbing patches are progressively introduced.

	250 Hz		500 Hz	
	Measured	Predicted	Measured	Predicted
No absorption	2.9%	1.8%	–	–
13 patches	2.8%	2.6%	2.6%	2.3%
26 patches	3.5%	3.2%	3.4%	3.1%
39 patches	4.7%	3.7%	4.3%	3.6%

Theoretically, the values with all 39 absorptive patches in Table VII should be the same as the values given in Table VI, whereas it can be seen that there is a significant difference. Different source and receiver locations were used for the measurements summarized in the two tables and the data in Table VII comes from a comparatively small number of measurements (12 source–receiver pairs).

Bartel and Magrab[23] found that rotating diffusing panels significantly reduced the scatter of reverberation time, whereas fixed diffusing panels had little effect. However, Balachandran and Robinson[26] show that fixed diffusers can substantially improve sound field diffusion. Sixteen fixed plastic diffusers (80 mm by 120 mm) were suspended in Model 1 and Table VIII lists the measured scatter of reverberation time and sound levels. The data in Table VIII without the diffusers should be the same as Tables VI and VII but, again, different source–receiver pairs have been used and there are significant differences. The addition of the diffusers reduces the scatter of reverberation time to slightly below the predicted values.

An illustration of the results presented in Table VIII can

TABLE VIII. Measurements in Model 1 with and without diffusing panels. Results are for the relative standard deviation of the reverberation time and the standard error of the reflected sound level.

	250 Hz	500 Hz
Relative S.D. of T_{20}:		
Without diffusers	5.7%	4.3%
With diffusers	3.3%	2.9%
Standard error of G_r:		
Without diffusers	0.52 dB	0.55 dB
With diffusers	0.52 dB	0.54 dB

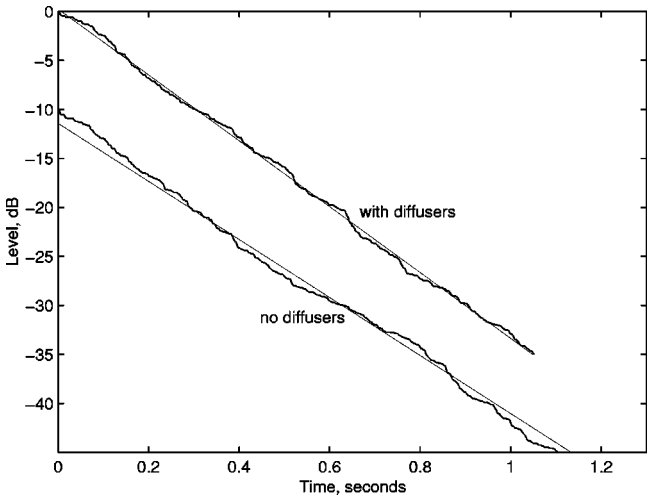

FIG. 11. A decay curve in Model 1 with and without diffusers. For ease of viewing, the curve for the model without diffusers is offset by −10 dB. The straight lines are the best-fit lines determined over the range −5 dB to −25 dB for each decay curve.

be made by plotting single decay curves. Figure 11 shows two decay curves for the same source–receiver pair, from the measurements summarized in Table VIII, with and without the diffusers present. For clarity, the curve without diffusers is offset by −10 dB. The figure also shows the best-fit lines determined over the range −5 dB to −25 dB, as used for determining the reverberation time. Without diffusers the decay curve is less linear with greater deviations from the best-fit line (the standard error from the best-fit line between −5 dB and −25 dB is 0.59 dB without diffusers and 0.37 dB with diffusers).

Therefore, for this particular source–receiver pair the automated calculation of reverberation time using these best-fit lines will be less accurate without the diffusers. This effect is considered to be the cause of the higher scatter of reverberation times without diffusers seen in Table VIII. This is also thought to be the reason for the scatter of reverberation time being above the predicted values for Model 1 in Tables VI and VII.

The consideration of reverberation time scatter is presented here as part of the investigation of sound level scatter. However, Table VIII shows that even when the reverberation time scatter significantly changes following the addition of diffusers, the scatter of sound levels remains largely unaffected. A similar result was found by Bartel and Magrab[21] who show that rotating diffusers substantially reduce the normalized standard deviation of reverberation time in the decaying sound field but have little effect on the scatter of steady-state sound levels.

IX. CONCLUSIONS

Revised theory has previously been shown to predict reflected sound levels in concert halls significantly more accurately than classical theory. Measurements of sound levels have been made in two scale models of proportionate spaces. To promote a diffuse sound field in these spaces, one model has nonparallel geometry and the other has acoustically scattering surfaces. Both models contain absorptive finishes to give average absorption coefficients ranging from 0.16 to 0.45. From these measurements it has been shown in all conditions tested that reflected sound levels decrease with distance from the source and revised theory is significantly more accurate than classical theory. The revised theory predictions are close to the best-fit lines through the data and it is concluded that it can be used for a calculation of the average behavior in proportionate spaces with diffuse sound fields. The magnitude of the revised theory effect is a function of the average absorption coefficient and the effect is therefore negligible in spaces such as a reverberation chambers which have very low average absorption coefficients, even when there is a highly absorbent sample on the floor.

The scatter of reflected sound levels measured in this investigation is significant. For spaces containing a moderate quantity of absorption, where the reflected sound level is correlated with the source–receiver distance, it is appropriate to use the standard error as a measure of scatter, rather than standard deviation. The scatter measured in the models is of a similar order to theoretical predictions but is consistently greater than them. However, it has been demonstrated that the theory does accurately predict the scatter of late sound levels for the part of the decays after the early reflections. Development of the theory is required to include the greater variation in reflected sound levels due to early reflections. A computer model analysis of the physical models gave a reduced scatter of predicted sound levels at lower frequencies. The use of a phase approximation in the computer model increased the scatter to a more realistic level but did not appear to improve the accuracy of individual values.

For these proportionate spaces, the measured scatter of reverberation time agrees well with predictions using theory proposed by Davy. An examination of this quantity in the two models suggested that the sound field in the model with nonparallel geometry was not as diffuse as in the model with scattering surfaces. The scatter of reverberation time in the model with nonparallel geometry was reduced by the addition of diffusing panels but this did not affect the scatter of sound levels.

ACKNOWLEDGMENTS

We are grateful for the assistance we have received from several people but in particular we would like to thank Michael Vorländer, Finn Jacobsen for drawing our attention to the previous work on sound level scatter, and Bengt-Inge Dalenbäck for his kind collaboration with the computer modeling and review of this paper. This research is funded by the UK Engineering and Physical Sciences Research Council.

[1] A.-C. Gade and J. H. Rindel, "Die Abstandsabhängigkeit vom Schallpegel in Konzertsälen," Fortschritte der Akustik-DAGA '85, 1985, pp. 434–438.
[2] M. Barron and L.-J. Lee, "Energy relations in concert auditoriums, 1," J. Acoust. Soc. Am. **84**, 618–628 (1988).
[3] M. Vorländer, "Revised relation between the sound power and the average sound pressure level in rooms and consequences for acoustic measurements," Acustica **81**, 332–343 (1995).
[4] J. J. Sendra, T. Zamarreño, and J. Navarro, "An analytical model for evaluating the sound field in Gothic-Mudejar churches," in *Computational Acoustic and its Environmental Applications II*, edited by C. A. Brebbia *et al.* (Computational Mechanics Publications, Southampton, 1997), pp. 139–148.

[5] E. Cirillo and F. Martellotta, ''An improved model to predict energy-based acoustic parameters in Apulian-Romanesque churches,'' Appl. Acoust. **64**, 1–23 (2003).
[6] M. Barron, ''Growth and decay of sound intensity in rooms according to some formulae of geometric acoustics theory,'' J. Sound Vib. **27**, 183–196 (1973).
[7] A. Magrini and P. Ricciardi, ''Churches as auditoria: Analysis of acoustical parameters for a better understanding of sound quality,'' Building Acoust. **10**, 135–158 (2003).
[8] N. Prodi, M. Marsilio, and R. Pompoli, ''On the prediction of reverberation time and strength in mosques,'' in *Proceedings of the 17th ICA*, Rome, 2001.
[9] M. Barron, ''Acoustic scale model testing over 21 years,'' Acoust. Bull. **22**, 5–12 (1997).
[10] M. Barron, ''Impulse testing techniques for auditoria,'' Appl. Acoust. **17**, 165–181 (1984).
[11] A. Lundeby, T. E. Vigran, H. Bietz, and M. Vorländer, ''Uncertainties of measurements in room acoustics,'' Acustica **81**, 344–355 (1995).
[12] ISO 9613-1:1993, ''Acoustics—Attenuation of sound during propagation outdoors—Part 1: Calculation of the absorption of sound by the atmosphere,'' International Organization for Standardization, Geneva, Switzerland, 1993.
[13] L. W. Sepmeyer, ''Computed frequency and angular distribution of the normal modes of vibration in rectangular rooms,'' J. Acoust. Soc. Am. **37**, 413–423 (1965).
[14] M. Vorländer and E. Mommertz, ''Definition and measurement of random-incidence scattering coefficients,'' Appl. Acoust. **60**, 187–199 (2000).
[15] ISO 3382:1997. ''Acoustics-Measurement of reverberation time of rooms with reference to other acoustical parameters,'' International Organization for Standardization, Geneva, Switzerland, 1997.
[16] D. Lubman, ''Fluctuations of sound with position in a reverberant room,'' J. Acoust. Soc. Am. **44**, 1491–1502 (1968).
[17] M. R. Schroeder, ''Effect of frequency and space averaging on the transmission responses of multimode media,'' J. Acoust. Soc. Am. **46**, 277–283 (1969).
[18] D. Lubman, ''Precision of reverberant sound power measurements,'' J. Acoust. Soc. Am. **56**, 523–533 (1974).
[19] J. L. Davy, I. P. Dunn, and P. Dubout, ''The variance of decay rates in reverberation rooms,'' Acustica **43**, 12–25 (1979).
[20] J. L. Davy, ''The variance of impulse decays,'' Acustica **44**, 51–56 (1980).
[21] J. L. Davy, ''The variance of decay rates at low frequencies,'' Appl. Acoust. **23**, 63–79 (1988).
[22] J. L. Davy and I. P. Dunn, ''The statistical bandwidth of Butterworth filters,'' J. Sound Vib. **115**, 539–549 (1987).
[23] T. E. Bartel and E. B. Magrab, ''Studies on the spatial variation of decaying sound fields,'' J. Acoust. Soc. Am. **63**, 1841–1850 (1978).
[24] J. P. Flenner, J. P. Guilhot, and C. Legros, ''Dispersion des measures de la durée de réverbération d'un local,'' Acustica **50**, 201–208 (1982).
[25] A. C. C. Warnock, ''Some practical aspects of absorption measurements in reverberation rooms,'' J. Acoust. Soc. Am. **74**, 1422–1432 (1983).
[26] C. G. Balachandran and D. W. Robinson, ''Diffusion of the decaying sound field,'' Acustica **19**, 245–257 (1967/68).